

Theory of bound-electron g factor in highly charged ions^{a)}

V.M. Shabaev¹, D.A. Glazov^{1,2,3}, G. Plunien³, and A.V. Volotka^{1,3†}

¹*Department of Physics, St. Petersburg State University, Ulianovskaya 1, Petrodvorets, St. Petersburg 198504, Russia*

²*SSC RF ITEP of NRC “Kurchatov Institute”, Bolshaya Cheremushkinskaya 25, Moscow, 117218, Russia*

³*Institut für Theoretische Physik, TU Dresden, Mommsenstrasse 13, Dresden, D-01062, Germany*

(Dated: 4 August 2015)

The paper presents the current status of the theory of bound-electron g factor in highly charged ions. The calculations of the relativistic, QED, nuclear recoil, nuclear structure, and interelectronic-interaction corrections to the g factor are reviewed. Special attention is paid to tests of QED effects at strong coupling regime and determinations of the fundamental constants.

^{a)}Invited paper published as part of the Proceedings of the Fundamental Constants Meeting, Eltville, Germany, February, 1-6, 2015.

I. INTRODUCTION

In the past two decades there has been a continuing interest in theoretical studies of the magnetic moments of highly charged ions. This interest was triggered by the first experiments on the g factor of H-like C¹ and O² and was supported by the recent measurements for some higher- Z ions^{3–5}. The comparison of the theoretical and experimental results has provided not only the most precise tests of quantum electrodynamics (QED) with middle- Z ions but has also led to the most precise determination of the electron mass in atomic mass units. It is anticipated that in the near future the measurements of the g factor will be extended to heavy ions, including few-electron ions of lead and uranium. From the theoretical side, to probe the QED effects with these measurements, in addition to accurate calculations of various contributions, one has to find some tricks to avoid the large uncertainties due to nuclear size and polarization effects. As was shown in Refs.^{6,7}, this can be done by studying specific differences of the g factors of H-, Li-, and B-like ions. Therefore, accurate calculations of all these ions are required to provide stringent tests of the theoretical methods employed for the g -factor calculations and to use these studies for determination of the fundamental constants. The present paper contains an overview of these calculations.

The relativistic units ($\hbar = c = m = 1$) are used throughout the paper.

II. THE g FACTOR OF H-LIKE IONS

The g factor of an ion can be defined as the ratio of the magnetic moment of the ion to its mechanical moment expressed in the Bohr's magnetons. Alternatively, it can be defined as the dimensionless coefficient in the linear part of the Zeeman splitting:

$$\Delta E = g\mu_0 \mathcal{H} M_J , \quad (1)$$

where $\mu_0 = |e|\hbar/(2mc)$ is the Bohr magneton and M_J is the angular momentum projection on the direction of the homogeneous magnetic field \mathcal{H} . The total theoretical value of the g factor of a hydrogenlike ion is given by a sum

$$g = g_D + \Delta g_{\text{QED}} + \Delta g_{\text{NR}} + \Delta g_{\text{NS}} + \Delta g_{\text{NP}} , \quad (2)$$

where g_D is the point-nucleus Dirac value, Δg_{QED} is the QED correction, and the last three terms denote the nuclear recoil (NR), nuclear size (NS), and nuclear polarization (NP) corrections, re-

spectively. The point-nucleus Dirac value can easily be evaluated analytically:

$$g_D = \frac{\kappa}{2j(j+1)} \left(\frac{2\kappa E}{m} - 1 \right), \quad (3)$$

where E is the Dirac energy for the point-charge nucleus and $\kappa = (-1)^{j+l+1/2}(j+1/2)$ is the angular-momentum-parity quantum number. For an ns state it yields⁸

$$\begin{aligned} g_D &= 2 + \frac{4E-m}{3m} \\ &= 2 - \frac{2(\alpha Z)^2}{3n^2} + \left(\frac{1}{2n} - \frac{2}{3} \right) \frac{(\alpha Z)^4}{n^3} + \dots, \end{aligned} \quad (4)$$

where the first term, 2, corresponds to the free-electron Dirac g factor and the other terms are the relativistic binding corrections. The QED correction can also be represented as a sum of the free-electron QED contribution and the binding-QED correction:

$$\Delta g_{\text{QED}} = \Delta g_{\text{free-QED}} + \Delta g_{\text{bind.-QED}}.$$

The free-electron g factor is given by

$$\begin{aligned} g_{\text{free}} &= 2 + \Delta g_{\text{free-QED}} + \Delta \\ &= 2 + 2 \left[A^{(2)} \frac{\alpha}{\pi} + A^{(4)} \left(\frac{\alpha}{\pi} \right)^2 + A^{(6)} \left(\frac{\alpha}{\pi} \right)^3 + \dots \right] + \Delta, \end{aligned} \quad (5)$$

where the Δ term denotes the sum of the hadronic and weak contributions. To date, the $A^{(2n)}$ coefficients have been calculated up to $n=5$ (see Refs.^{9,10} and references therein). With these calculations, the theoretical accuracy of the free-electron g factor is presently limited by the accuracy of the fine structure constant α . As the result, the comparison of the theory and the corresponding free-electron g -factor experiment¹¹ has provided the most precise determination of α ^{9,10}.

A. Binding-QED corrections

For an ns state, the binding-QED correction to the lowest order in αZ and to all orders in α is given by¹²⁻¹⁷:

$$\Delta g_{\text{bind.-QED}}^{(\text{l.o.})} = \Delta g_{\text{free-QED}} \frac{(\alpha Z)^2}{6n^2}, \quad (6)$$

where $\Delta g_{\text{free-QED}}$ is the total free-electron QED correction. The formula (6) can be derived using the Pauli operator

$$H_{\text{rad}} = \frac{|e|}{2m} \frac{g_{\text{free}} - 2}{2} [\beta(\boldsymbol{\sigma} \cdot \mathcal{H}) - i\beta(\boldsymbol{\alpha} \cdot \mathcal{E})], \quad (7)$$

where $\mathcal{E} = |e|Z\mathbf{r}/(4\pi r^3)$, α and β are the Dirac matrices. The expectation value of H_{rad} is evaluated with the Dirac wave function of the electron that accounts for the interaction with the homogeneous magnetic field to first order in \mathcal{H} . The first-order correction to the electronic wave function due to the interaction with the magnetic field is easily obtained using the generalized virial relations for the Dirac equation^{18,19}.

The evaluation of the QED correction to all orders in the αZ parameter is a much more difficult problem. This correction consists of two contributions: the self-energy (SE) and vacuum-polarization (VP) ones. The corresponding Feynman diagrams are given in Figs. 1 and 2, respectively, where the dashed line terminated by a triangle represents the interaction with the external magnetic field. For the ground $1s$ state the SE correction to all orders in αZ was first evaluated in Refs.^{20–23}. However, the first experiments on the g factor of H-like C¹ and O² demanded more precise calculations of this correction. The required accuracy was achieved in Refs.^{24,25} and further improved in Refs.^{26,27}.

The VP contributions are generally represented by a sum of the Uehling and the Wichmann-Kroll terms. The Uehling term is defined by the lowest-order contributions in the expansion of the fermion loops in powers of the electron-nucleus interaction, that are not ruled out by the Furry theorem. In the Uehling approximation only the electric-loop diagrams contribute to the g factor value. These are the first two diagrams in Fig. 2. As to the magnetic-loop VP contribution (the third diagram in Fig. 2), it vanishes in the Uehling approximation. The evaluation of the Uehling and Wichmann-Kroll corrections to all orders in αZ was considered in Refs.^{21–23}. For the point-charge nucleus, the Uehling contribution can be evaluated analytically²⁸. The evaluation of the magnetic-loop Wichmann-Kroll part to the lowest order in αZ for an ns state gives²⁹

$$\Delta g_{\text{VP}}^{\text{magn}} = \frac{7}{216} \frac{\alpha(\alpha Z)^5}{n^3}. \quad (8)$$

The next-to-leading contribution of magnetic loop was calculated in Ref.³⁰.

The two-loop QED correction to the order $\alpha^2(\alpha Z)^2$ for an ns state is determined by Eq. (6). The evaluation of this correction to the order $\alpha^2(\alpha Z)^4$, performed in Refs.^{31,32}, yields

$$\begin{aligned} \Delta g_{\text{two-loop}}^{(\text{h.o.})} = & \left(\frac{\alpha}{\pi}\right)^2 \frac{(\alpha Z)^4}{n^3} \left\{ \frac{28}{9} \ln[(\alpha Z)^{-2}] + \frac{258917}{19440} - \frac{4}{9} \ln k_0 \right. \\ & - \frac{8}{3} \ln k_3 + \frac{113}{810} \pi^2 - \frac{379}{90} \pi^2 \ln 2 + \frac{379}{60} \zeta(3) \\ & \left. + \frac{1}{n} \left[-\frac{985}{1728} - \frac{5}{144} \pi^2 + \frac{5}{24} \pi^2 \ln 2 - \frac{5}{16} \zeta(3) \right] \right\}, \end{aligned} \quad (9)$$

where $\zeta(s)$ is the Riemann zeta function, $\ln k_0(1s) = 2.984128556$, $\ln k_0(2s) = 2.811769893$, $\ln k_3(1s) = 3.272806545$, and $\ln k_3(2s) = 3.546018666$. Finally, we note that the calculations of two-loop QED corrections with the closed fermion loops were considered for the $1s$ state in Refs.^{33,34}.

B. Nuclear recoil corrections

It is known³⁵ that for an ns state the nuclear recoil correction to the g factor is of pure relativistic origin. This means that, in contrast to the p states, its expansion in the parameter αZ starts with the $(\alpha Z)^2$ terms, which can be derived from the Breit equation. An extension of this equation, including the interaction due to the anomalous magnetic moment of free electron, allows also to account for the lowest-order radiative recoil effect. As the result, the nuclear recoil correction to the orders up to $(\alpha Z)^2$, (α/π) , and $(m/M)^2$ is given by^{13–15,36–38}

$$\Delta g_{\text{NR}}^{(1.\text{o.})} = \frac{(\alpha Z)^2}{n^2} \left[\frac{m}{M} - (1+Z) \left(\frac{m}{M} \right)^2 \right] + \frac{\alpha (\alpha Z)^2}{\pi n^2} \left[-\frac{1}{3} \frac{m}{M} + \frac{3-2Z}{6} \left(\frac{m}{M} \right)^2 \right], \quad (10)$$

where M is the nuclear mass. It should be noted that this correction does not depend on the nuclear spin^{14,15,37,38}.

To evaluate the nuclear recoil correction for high- Z ions, we need first to derive the exact αZ -dependence formula for the recoil effect, at least to the first order in m/M . The desired formula was derived in Ref.³⁹. According to this formula, which was also confirmed in Ref.⁴⁰, the recoil correction to the g factor to the first order in m/M and to all orders in αZ is given by ($e < 0$)

$$\Delta g_{\text{NR}} = \frac{1}{\mu_0 m_a} \frac{i}{2\pi M} \int_{-\infty}^{\infty} d\omega \left[\frac{\partial}{\partial \mathcal{H}} \langle \tilde{a} | [p^k - D^k(\omega) + eA_{\text{cl}}^k] \times \tilde{G}(\omega + \tilde{E}_a) [p^k - D^k(\omega) + eA_{\text{cl}}^k] | \tilde{a} \rangle \right]_{\mathcal{H}=0}. \quad (11)$$

Here m_a is the angular momentum projection of the state under consideration, $\mathbf{A}_{\text{cl}} = [\mathcal{H} \times \mathbf{r}] / 2$ is the vector potential of the homogeneous magnetic field \mathcal{H} directed along the z axis, $p^k = -i\nabla^k$ is the momentum operator, $D^k(\omega) = -4\pi\alpha Z\alpha^l D^{lk}(\omega)$,

$$D^{il}(\omega, \mathbf{r}) = -\frac{1}{4\pi} \left\{ \frac{\exp(i|\omega|r)}{r} \delta_{il} + \nabla^i \nabla^l \frac{(\exp(i|\omega|r) - 1)}{\omega^2 r} \right\} \quad (12)$$

is the transverse part of the photon propagator in the Coulomb gauge. All the quantities marked with a tilde (the wave function, the energy, and the Coulomb Green function $\tilde{G}(\omega) = \sum_{\tilde{n}} |\tilde{n}\rangle \langle \tilde{n}| [\omega -$

$\tilde{E}_n(1 - i0)]^{-1}$) are assumed to be calculated in presence of the magnetic field \mathcal{H} . For the practical calculations, it is convenient to represent the expression (11) as a sum of a lower-order term and a higher-order term, $\Delta g_{\text{NR}} = \Delta g_{\text{NR}}^{(\text{l.o.})} + \Delta g_{\text{NR}}^{(\text{h.o.})}$, where

$$\begin{aligned}\Delta g_{\text{NR}}^{(\text{l.o.})} &= \frac{1}{\mu_0 m_a} \frac{1}{2M} \left[\frac{\partial}{\partial \mathcal{H}} \langle \tilde{a} | \left\{ \mathbf{p}^2 - \frac{\alpha Z}{r} [(\boldsymbol{\alpha} \cdot \mathbf{p}) + (\boldsymbol{\alpha} \cdot \mathbf{n})(\mathbf{n} \cdot \mathbf{p})] \right\} | \tilde{a} \rangle \right]_{\mathcal{H}=0} \\ &\quad - \frac{1}{m_a M} \frac{m}{M} \langle a | \left([\mathbf{r} \times \mathbf{p}]_z - \frac{\alpha Z}{2r} [\mathbf{r} \times \boldsymbol{\alpha}]_z \right) | a \rangle ,\end{aligned}\quad (13)$$

$$\begin{aligned}\Delta g_{\text{NR}}^{(\text{h.o.})} &= \frac{1}{\mu_0 m_a} \frac{i}{2\pi M} \int_{-\infty}^{\infty} d\omega \left[\frac{\partial}{\partial \mathcal{H}} \langle \tilde{a} | \left(D^k(\omega) - \frac{[p^k, V]}{\omega + i0} \right) \right. \\ &\quad \left. \times \tilde{G}(\omega + \tilde{E}_a) \left(D^k(\omega) + \frac{[p^k, V]}{\omega + i0} \right) | \tilde{a} \rangle \right]_{\mathcal{H}=0} ,\end{aligned}\quad (14)$$

where $V(r) = -\alpha Z/r$ is the Coulomb potential of the nucleus and $\mathbf{n} = \mathbf{r}/r$. The low-order term can be evaluated analytically employing the generalized virial relations^{18,19}. This yields³⁹

$$\Delta g_{\text{NR}}^{(\text{l.o.})} = -\frac{m}{M} \frac{2\kappa^2 E^2 + \kappa m E - m^2}{2m^2 j(j+1)} ,\quad (15)$$

where E is the Dirac energy. To the two lowest orders in αZ , we get

$$\Delta g_{\text{NR}}^{(\text{l.o.})} = -\frac{m}{M} \frac{1}{j(j+1)} \left[\kappa^2 + \frac{\kappa}{2} - \frac{1}{2} - \left(\kappa^2 + \frac{\kappa}{4} \right) \frac{(\alpha Z)^2}{n^2} \right] .\quad (16)$$

For the $1s$ state, the exact formula (15) takes the form:

$$\Delta g_{\text{NR}}^{(\text{l.o.})} = \frac{m}{M} (\alpha Z)^2 - \frac{m}{M} \frac{(\alpha Z)^4}{3[1 + \sqrt{1 - (\alpha Z)^2}]^2} .$$

The higher-order term can be represented as

$$\Delta g_{\text{NR}}^{(\text{h.o.})} = \frac{m}{M} \frac{(\alpha Z)^5}{n^3} P(\alpha Z) .$$

The numerical evaluation of the function $P(\alpha Z)$ for the $1s$ state was performed in Ref.⁴¹.

C. Nuclear size and polarization corrections

The finite nuclear size correction to the g factor can be calculated numerically (see, e.g. Refs.^{22,23}). The perturbative evaluation of this correction to two lowest orders in αZ yields for an ns state⁴²:

$$\begin{aligned}\Delta g_{\text{NS}} &= \frac{8}{3n^3} (\alpha Z)^4 m^2 \langle r^2 \rangle_{\text{nuc}} \left[1 + (\alpha Z)^2 \left(\frac{1}{4} + \frac{12n^2 - n - 9}{4n^2(n+1)} \right. \right. \\ &\quad \left. \left. + 2\psi(3) - \psi(2+n) - \frac{\langle r^2 \ln(2\alpha Z mr/n) \rangle_{\text{nuc}}}{\langle r^2 \rangle_{\text{nuc}}} \right) \right] ,\end{aligned}\quad (17)$$

where $\psi(x) = \frac{d}{dx} \ln \Gamma(x)$. The first term in the right-hand side of the equation (17) was first derived in Ref.⁴³. An approximate formula which expresses the nuclear size correction to the g factor in terms of the corresponding correction to the binding energy was derived in Ref.⁴⁴. The dependence of the nuclear size correction on the nuclear deformation parameters was studied in Ref.⁴⁵.

The nuclear polarization correction to the g factor is defined by the Feynman diagrams presented in Fig. 3. In these diagrams the double, thick, and wavy lines correspond to the electron, nucleus, and photon propagators, respectively. The dashed line ended by a triangle denotes the interaction of electron with the external magnetic field. The evaluations of these diagrams for some middle- and high- Z ions were performed in Refs.^{46,47}. In addition to the nuclear polarization contribution, there exists also a nuclear magnetic susceptibility correction, which is defined by the one-photon exchange diagrams with the magnetic interaction attached to the nuclear line. The calculations performed in Refs.^{47,48} showed that this correction is rather small.

D. Comparison of theory and experiment: determination of the electron mass

First high-precision measurement of the g factor with highly charged ions was accomplished for $^{12}\text{C}^{5+}$ in Ref.¹. The experiment was performed using a single ion confined in a Penning ion trap. The experimental value of the g factor was presented as

$$g_{\text{exp}} = 2(q/|e|)(m/M_{\text{ion}})(\omega_L/\omega_c), \quad (18)$$

where $\omega_c = (q/M_{\text{ion}})\mathcal{H}$ is the cyclotron frequency, $\omega_L = \Delta E/\hbar$ is the Larmor precession frequency, M_{ion} is the ion mass, and q is the ion charge. The experimental accuracy of the ω_L/ω_c ratio was so high that the uncertainty of g_{exp} was mainly due to the uncertainty of the value of the electron mass. This stimulated high-precision calculations of the nuclear recoil and one-loop QED corrections^{24,39,41}. As the result, the theoretical accuracy was significantly improved, and the comparison of the theory and the experiment led to a four-times improvement of the accuracy of the electron mass^{24,49,50}. Later², the g factor of $^{16}\text{O}^{7+}$ was measured to a similar accuracy. The value of the electron mass derived from the comparison of this experiment with the related theory agreed with the determination on $^{12}\text{C}^{5+}$.

In Refs.^{3,4} the g factor of $^{28}\text{Si}^{13+}$ was measured to amount $g_{\text{exp}} = 1.99534895910(7)(7)(80)$, where the first and second errors represent the statistical and systematic uncertainties, while the

third one is due to the current uncertainty of the electron mass. The theoretical contributions to the g factor of $^{28}\text{Si}^{13+}$ are presented in Table I. These experiment and theory provide the most accurate to-date test of bound-state QED with middle- Z ions. The current theoretical uncertainty, which is two times bigger than the experimental one, is mainly defined by uncalculated two-loop QED corrections of order $\alpha^2(\alpha Z)^5$ and higher. This uncertainty can be reduced in a combination of the corresponding theoretical and experimental values for two different H-like ions. This idea was explored in Ref.⁵, where the high-precision measurements of the g factors of $^{12}\text{C}^{5+}$ and $^{28}\text{Si}^{13+}$ were combined with the theory to extract a new value of the electron mass which is by a factor of 13 more precise than the previously accepted value. Namely, the experimental value of the g factor, which is determined by

$$g_{\text{exp}} = 2(Z - 1)(m/M_{\text{ion}})(\omega_L/\omega_c), \quad (19)$$

was fitted as

$$g_{\text{exp}} = g_{\text{theor}}^* + (\alpha/\pi)^2(\alpha Z)^5 b_{50}, \quad (20)$$

where g_{theor}^* is the theoretical value which incorporates only the known contributions. Then, the equations (19)-(20) give

$$\left(\frac{\alpha}{\pi}\right)^2 (6\alpha)^5 b_{50} = 2(6 - 1) \frac{m}{M_{^{12}\text{C}^{5+}}} \left(\frac{\omega_L}{\omega_c}\right)_{^{12}\text{C}^{5+}} - g_{\text{theor}}^*[^{12}\text{C}^{5+}], \quad (21)$$

$$\left(\frac{\alpha}{\pi}\right)^2 (14\alpha)^5 b_{50} = 2(14 - 1) \frac{m}{M_{^{28}\text{Si}^{13+}}} \left(\frac{\omega_L}{\omega_c}\right)_{^{28}\text{Si}^{13+}} - g_{\text{theor}}^*[^{28}\text{Si}^{13+}]. \quad (22)$$

The solution of these equations yields⁵ $m = 0.000548579909067(14)(9)(2)$ u and $b_{50} = -4.0(5.1)$. The indicated uncertainties include also an uncertainty due to the omitted higher-order QED corrections, $\sim (\alpha/\pi)^2(\alpha Z)^6 \ln^k[(\alpha Z)^{-2}]$, in Eq. (20).

III. THE g FACTOR OF LI-LIKE IONS

The theoretical accuracy of the g factor for high- Z ions is strongly limited by the uncertainties of the nuclear effects. In particular, it makes impossible tests of the two-loop QED contributions by the direct comparison of the theory and experiment on the g factor of H-like lead or uranium ions (see, e.g., Refs.^{6,47}). To extend the region accessible to the QED tests with the g -factor experiments, it was proposed⁶ to study a specific difference of the g factors of H- and Li-like ions of the same isotope:

$$g' = g_{(1s)^2 2s} - \xi g_{1s}, \quad (23)$$

where g_{1s} and $g_{(1s)2s}$ are the ground-state g factors of H- and Li-like ions, respectively, and the parameter ξ is chosen to cancel the nuclear size effect. It can be shown⁶ that both the parameter ξ and the difference g' are very stable with respect to variations of the nuclear structure parameters. As the result, this difference can be calculated to a much higher accuracy than each of the g factors. This stimulated significant efforts in calculations of the g factor of Li-like ions^{51–56}.

The theoretical value of the g factor of a Li-like ion can be written as

$$g = g_{\text{one-elec}} + \Delta g_{\text{int}} + \Delta g_{\text{scr.-QED}}, \quad (24)$$

where $g_{\text{one-elec}}$ incorporates all the one-electron contributions, which were considered in the previous section, Δg_{int} is the interelectronic-interaction contribution, and $\Delta g_{\text{scr.-QED}}$ denotes the screened QED correction. The interelectronic-interaction and screened QED corrections are evaluated using the perturbation theory in the parameter $1/Z$.

The interelectronic-interaction contribution can be represented as

$$\Delta g_{\text{int}} = \Delta g_{\text{int}}^{(1)} + \Delta g_{\text{int}}^{(2)} + \Delta g_{\text{int}}^{(3+)}, \quad (25)$$

where the terms

$$\Delta g_{\text{int}}^{(1)} = \frac{1}{Z}(\alpha Z)^2 B(\alpha Z), \quad (26)$$

$$\Delta g_{\text{int}}^{(2)} = \frac{1}{Z^2}(\alpha Z)^2 C(\alpha Z) \quad (27)$$

denote the contributions of the first and second orders in $1/Z$, which are defined by the Feynman diagrams depicted in Figs. 4 and 5, respectively. The term $\Delta g_{\text{int}}^{(3+)}$ includes all the interelectronic-interaction corrections of the third and higher orders in $1/Z$. In formulas (26) and (27) the factor $(\alpha Z)^2$ accounts for the relativistic origin of the interelectronic-interaction effects on the g factor. The function $B(\alpha Z)$ was first evaluated in Ref.⁶. The exact calculation of the function $C(\alpha Z)$ is a much more difficult task. This calculation within the rigorous QED approach was performed in Ref.⁵⁶. In addition, in that paper the contribution $\Delta g_{\text{int}}^{(3+)}$ was evaluated within the Breit approximation using the large-scale configuration-interaction Dirac-Fock-Sturm method^{51,57–59}. To accelerate the convergence of the $1/Z$ expansion, the calculations were performed starting with an effective spherically symmetric potential which partly accounts for the electron-electron interaction effects. To avoid the double counting of these effects, the related subtraction was carried out in the higher orders of the perturbation theory.

The calculation of the one-loop QED corrections to the g factor of Li-like ions with an effective local potential, which partly accounts for the screening effect, was first performed in Ref.⁵². The

screened SE corrections and the Uehling part of the screened VP corrections, presented in Figs. 6 and 7, respectively, were evaluated in Refs.^{53,54,56}. As in the case of the two-photon exchange diagrams, the calculations were accomplished starting with an effective local potential.

In Table II the theoretical prediction for the g factor of $^{28}\text{Si}^{11+}$ is compared with the recent experiment⁶⁰. To date, these experiment and theory provide the most accurate test of many-electron QED effects with middle- Z ions.

IV. FUTURE PROSPECTS

A. Tests of QED and determination of the nuclear charge radii

The measurements of the g factors of heavy few-electron ions, that are anticipated in the near future at the HITRAP facilities in Darmstadt and at MPIK in Heidelberg, will provide the most precise tests of the magnetic sector of QED at strong electric field. Moreover, the study of the g factor can give a unique opportunity to test QED effects with highly charged ions beyond the external field approximation (the Furry picture of QED). The most appropriate way to access bound-state QED beyond the Furry picture would consist in studying the isotope shifts of the g factor of highly charged ions. In Table III we present the theoretical contributions to the isotope shift of H-like calcium. The nuclear size effect was evaluated with the nuclear charge radii taken from Ref.⁶¹. The uncertainty of this correction includes both the nuclear radius and shape variation effects. As one can see from the table, the current theoretical uncertainty of the $^{40}\text{Ca}^{19+} - ^{48}\text{Ca}^{19+}$ isotope shift is about 9% of the QED nuclear recoil contribution. This would allow tests of bound-state QED beyond the external field approximation with highly charged ions, provided the corresponding shift is measured to the required accuracy. Alternatively, the study of the isotope shift can provide a determination of the nuclear-charge-radius difference to a high precision.

B. Determination of the nuclear magnetic moments

The extention of the g factor measurements to ions with non-zero nuclear spin would give an access to the nuclear magnetic moments⁶². To the lowest order, the g factor of an H-like ion with

a nonzero nuclear spin is given by (see, e.g., Ref.³⁵):

$$g_{\text{ion}} = g_D \frac{F(F+1) + j(j+1) - I(I+1)}{2F(F+1)} - \frac{m}{m_p} g_N \frac{F(F+1) + I(I+1) - j(j+1)}{2F(F+1)}, \quad (28)$$

where F is the total angular momentum of the ion, j and I are the electronic and nuclear angular momenta, respectively, g_D is the Dirac value of the electronic g factor given by Eq. (3), g_N is the nuclear g factor, and m_p is the proton mass. Various corrections to Eq. (28) for H- and Li-like ions as well as the corresponding corrections to the Breit-Rabi formula, which describes the Zeeman effect on the hyperfine-structure levels, were derived in Refs.^{63–68}. As was discussed in detail in Ref.⁶⁹, due to the absence of an uncertainty caused by the diamagnetic shielding, these studies can provide a determination of the nuclear magnetic moment with unprecedented accuracy.

C. Access to the nonlinear Zeeman effect

The laser-microwave double-resonance technique^{69–73} allows precise measurements of the Zeeman splittings of fine- and hyperfine-structure levels in a Penning trap. This, apart from the linear Zeeman effect, provides an access to the second- and third-order Zeeman effect with highly charged ions. The influence of the higher-order Zeeman effects on the fine-structure levels in boronlike argon was studied in Refs.^{72,74}. The related experiments are currently under preparation at GSI (Darmstadt).

D. Determination of the fine structure constant

Finally, let us discuss a possibility of an independent determination of the fine structure constants from the g factor experiments with heavy ions. For middle- and high- Z ions the g factor depends on α mainly via the relativistic binding correction in the Dirac formula (3). It follows that the uncertainty of such a determination can be estimated by

$$\frac{\delta\alpha}{\alpha} \sim \frac{1}{(\alpha Z)^2} \sqrt{(\delta g_{\text{exp}})^2 + (\delta g_{\text{th}})^2}, \quad (29)$$

where δg_{exp} and δg_{th} are the uncertainties of the experimental and theoretical values of the g factor, respectively. As one can see, at the given values of δg_{exp} and δg_{th} the uncertainty of α decreases with Z as $1/Z^2$. A simple evaluation shows that to get α to the same accuracy as it was obtained

from the free-electron g factor experiment one should measure the g factor of H-like Pb to an uncertainty of about 3×10^{-10} , provided the theoretical value is known to the required precision. This uncertainty is by three orders of magnitude bigger than the corresponding uncertainty in the free-electron g factor experiment. This would seem very promising, if we could calculate the theoretical value of the bound-electron g factor to the required accuracy. Unfortunately, the accuracy of the bound-electron g factor is strongly restricted by the nuclear size and polarization effects. The use of the difference (23) of the g factors of H- and Li-like ions, which can be calculated to a very high accuracy, does not help since the α -dependent term is significantly reduced in this difference. Instead, one should consider the corresponding difference of the g factors of H- and B-like ions of lead⁷:

$$g' = g_{(1s)^2(2s)^22p_{1/2}} - \xi g_{1s}, \quad (30)$$

where $g_{(1s)^2(2s)^22p_{1/2}}$ and g_{1s} are the g factors of $^{208}\text{Pb}^{77+}$ and $^{208}\text{Pb}^{81+}$, respectively, and the parameter ξ must be chosen to cancel the nuclear size effect. In Ref.⁷ it was shown that both the parameter ξ and the difference g' are very stable with respect to variations of the nuclear structure parameters. At the same time the α -dependent term is reduced in this difference by about 4% only. In Table IV we give the uncertainties of g' due to the uncertainty of the current value of α^{10} and due to the nuclear polarization effect⁴⁷, which sets the ultimate accuracy limit up to which this difference can be calculated. As one can see from the table, the uncertainty caused by the current value of α is slightly bigger than the nuclear polarization limit. This means that the method has a potential to provide a determination of α to an accuracy comparable to one obtained from the free-electron g factor study. To achieve the required accuracy from the theoretical side, we need to calculate all two-loop and, at least approximately, three-loop QED corrections. While the calculation of the two-loop corrections seems quite realistic with the most elaborated to-date methods^{75,76}, the evaluation of the three-loop contributions requires development of essentially new methods.

V. CONCLUSION

In this paper we have reviewed the calculations of the various contributions to the g factor of highly charged ions. The experimental and theoretical investigations of the g factors have already allowed the most stringent tests of one- and many-electron QED effects with middle- Z ions and provided the most precise determination of the electron mass. The theoretical predictions for

TABLE I. Theoretical contributions to the g factor of H-like Si.

Dirac value (point nucleus)	1.993 023 571 6
Free QED	0.002 319 304 4
Binding QED	0.000 005 855 6(17)
Nuclear recoil	0.000 000 205 9
Nuclear size	0.000 000 020 5
Total theory	1.995 348 958 0(17)
Experiment ⁴	1.995 348 959 10(7)(7)(80)

TABLE II. Theoretical contributions to the g factor of Li-like Si.

Dirac value (point nucleus)	1.998 254 751
Free QED	0.002 319 304
Binding QED	0.000 000 987(6)
Interelectronic interaction	0.000 314 809(6)
Nuclear recoil	0.000 000 039(1)
Nuclear size	0.000 000 003
Total theory	2.000 889 892(8)
Experiment ⁶⁰	2.000 889 890(2)

heavy ions suffer from the large uncertainties due to the nuclear structure effects. This prevents high-precision tests of bound-state QED on the two-loop level and restricts the possibilities for determinations of the fundamental constants by the direct comparison of the theory and experiment for heavy ions. It has been shown, however, that this restriction can be overcomed by studying the specific differences of the g factors of H-, Li-, and B-like ions. The study of these differences should allow tests of bound-state QED at strong fields and provide an independent determination of the fine structure constant. The investigations of the isotope shifts of the g factor with highly charged ions can give a unique opportunity to probe QED beyond the Furry picture. They can also be used for a precise determination of the nuclear-charge-radius differences. The study of the g factors of highly charged ions with non-zero nuclear spin will provide determinations of the nuclear magnetic moments with unprecedented accuracy.

TABLE III. Theoretical contributions to the isotope shift of the g factor of H-like calcium: ${}^{40}\text{Ca}^{19+}$ – ${}^{48}\text{Ca}^{19+}$.

Nuclear recoil: non-QED $\sim m/M$	0.000 000 048 657
Nuclear recoil: non-QED $\sim (m/M)^2$	-0.000 000 000 026(2)
Nuclear recoil: QED $\sim m/M$	0.000 000 000 904
Nuclear recoil: QED $\sim \alpha(m/M)$	-0.000 000 000 038(3)
Nuclear size	0.000 000 000 032(78)
Total theory	0.000 000 049 529(78)

TABLE IV. The uncertainties of g' , defined by Eq. (30), for Pb due to the current uncertainty of α and the nuclear polarization effect.

Effect	$\delta g'$	$\delta g'/g'$
$1/\alpha = 137.035999173(35)$	0.4×10^{-10}	0.7×10^{-10}
Nuclear polarization	0.3×10^{-10}	0.5×10^{-10}

ACKNOWLEDGMENTS

This work was supported by RFBR (Grants No. 13-02-00630 and 14-02-31316), by SPbSU (Grants No. 11.38.269.2014 and No. 11.38.237.2015), by DFG, and by the FAIR–Russia Research Center.

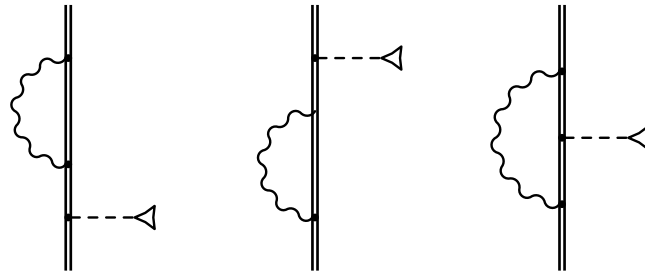


FIG. 1. The self-energy corrections to the bound-electron g factor.

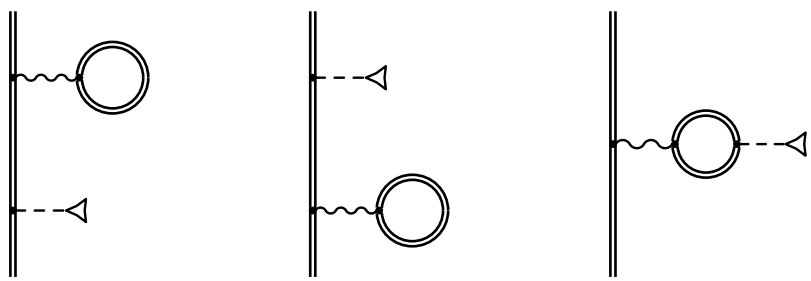


FIG. 2. The vacuum-polarization corrections to the bound-electron g factor.

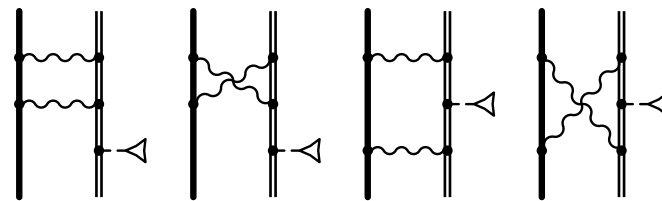


FIG. 3. The nuclear-polarization corrections to the bound-electron g factor.

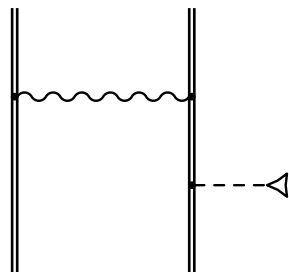


FIG. 4. The one-photon-exchange correction to the bound-electron g factor.

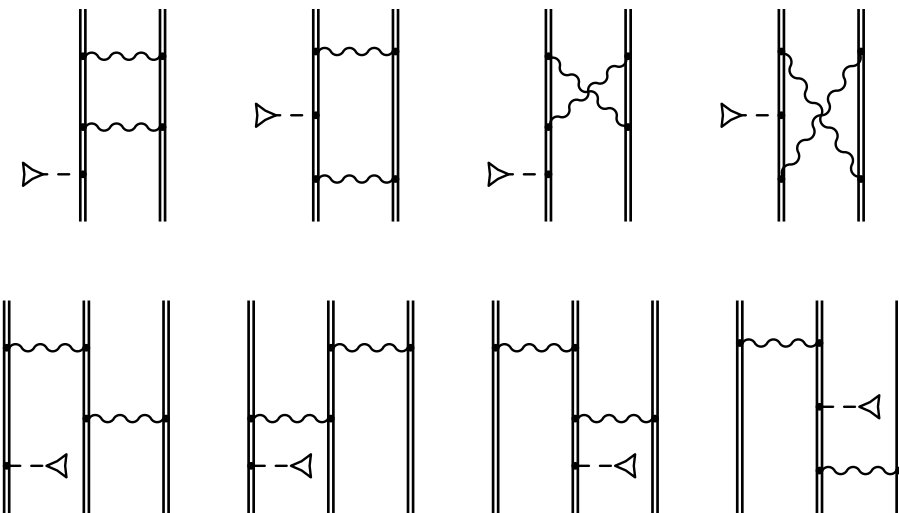


FIG. 5. The two-photon-exchange corrections to the bound-electron g factor.

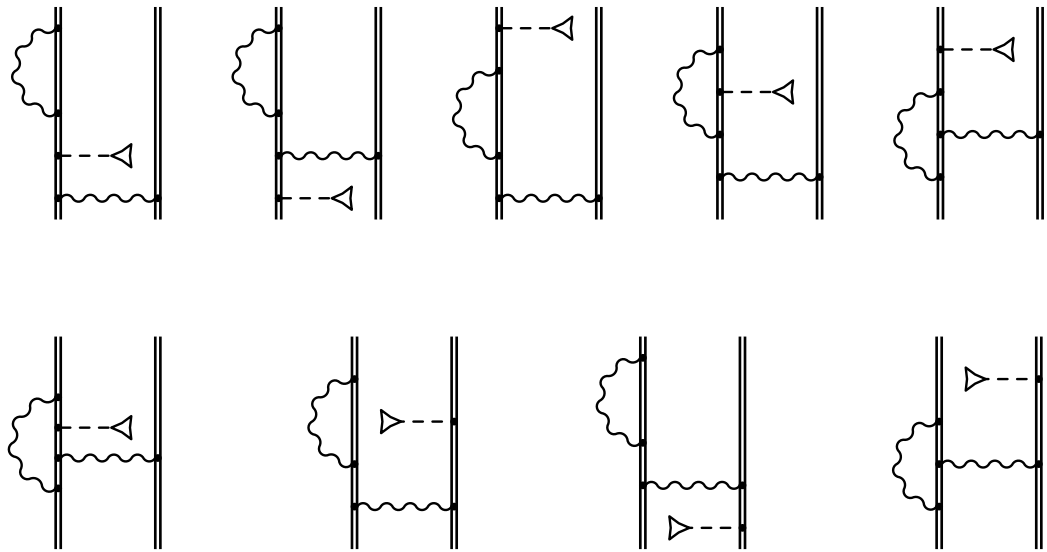


FIG. 6. The screened SE corrections to the bound-electron g factor.

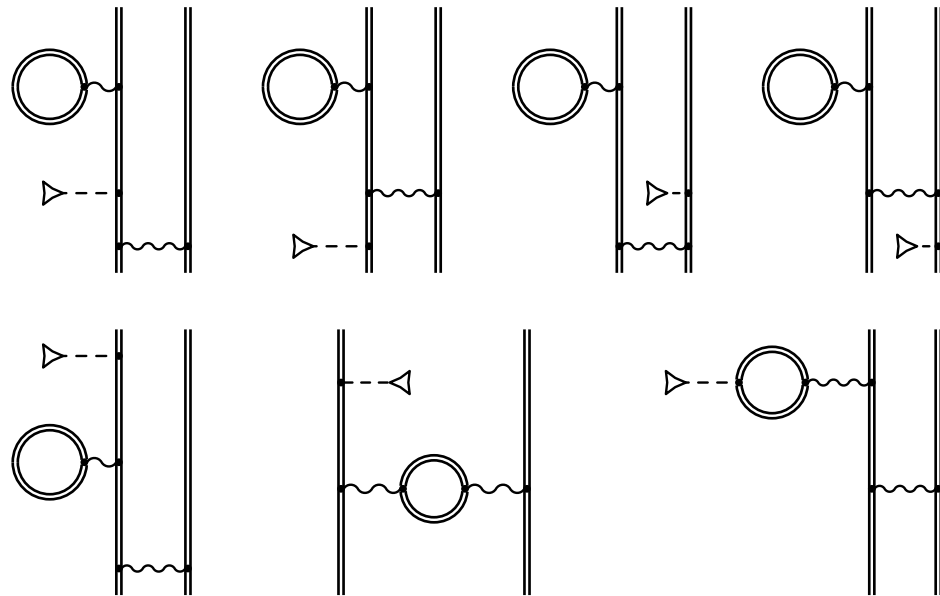


FIG. 7. The screened VP corrections to the bound-electron g factor.

REFERENCES

- ¹H. Häffner, T. Beier, N. Hermanspahn, H.-J. Kluge, W. Quint, S. Stahl, J. Verdú, and G. Werth, Phys. Rev. Lett. **85**, 5308 (2000).
- ²J. Verdú, S. Djekić, S. Stahl, T. Valenzuela, M. Vogel, G. Werth, T. Beier, H.-J. Kluge, and W. Quint, Phys. Rev. Lett. **92**, 093002 (2004).

- ³S. Sturm, A. Wagner, B. Schabinger, J. Zatorski, Z. Harman, W. Quint, G. Werth, C. H. Keitel, and K. Blaum, Phys. Rev. Lett. **107**, 023002 (2011).
- ⁴S. Sturm, A. Wagner, M. Kretzschmar, W. Quint, G. Werth, and K. Blaum, Phys. Rev. A **87**, 030501(R) (2013).
- ⁵S. Sturm, F. Köhler, J. Zatorski, A. Wagner, Z. Harman, G. Werth, W. Quint, C. H. Keitel, and K. Blaum, Nature **506**, 467 (2014).
- ⁶V. M. Shabaev, D. A. Glazov, M. B. Shabaeva, V. A. Yerokhin, G. Plunien, and G. Soff, Phys. Rev. A **65**, 062104 (2002).
- ⁷V. M. Shabaev, D. A. Glazov, N. S. Oreshkina, A. V. Volotka, G. Plunien, H.-J. Kluge, and W. Quint, Phys. Rev. Lett. **96**, 253002 (2006).
- ⁸G. Breit, Nature **122**, 649 (1928).
- ⁹T. Aoyama, M. Hayakawa, T. Kinoshita, and M. Nio, Phys. Rev. Lett. **109**, 111807 (2012).
- ¹⁰T. Kinoshita, International Journal of Modern Physics A **29**, 1430003 (2014).
- ¹¹D. Hanneke, S. Fogwell, and G. Gabrielse, Phys. Rev. Lett. **100**, 120801 (2008).
- ¹²H. Grotch, Phys. Rev. A **2**, 1605 (1970).
- ¹³R. Faustov, Phys. Lett. B **33**, 422 (1970).
- ¹⁴F. E. Close and H. Osborn, Phys. Lett. B **34**, 400 (1971).
- ¹⁵M. I. Eides and H. Grotch, Ann. Phys. (N.Y.) **260**, 191 (1997).
- ¹⁶A. Czarnecki, K. Melnikov, and A. Yelkhovsky, Phys. Rev. A **63**, 012509 (2000).
- ¹⁷S. G. Karshenboim, *The g Factor of a Bound Electron in a Hydrogen-Like Atom* (in The Hydrogen Atom, Ed. by S.G. Karshenboim *et al.*, p. 651, Springer, Berlin, 2001).
- ¹⁸V. M. Shabaev, J. Phys. B **24**, 4479 (1991).
- ¹⁹V. M. Shabaev, *Virial relations for the Dirac equation and their applications to calculations of hydrogen-like ions* (in Precision Physics of Simple Atomic Systems, Ed. by S. G. Karshenboim and V. B. Smirnov, p. 97, Springer-Verlag, Berlin, 2003).
- ²⁰S. A. Blundell, K. T. Cheng, and J. Sapirstein, Phys. Rev. A **55**, 1857 (1997).
- ²¹H. Persson, S. Salomonson, P. Sunnergren, and I. Lindgren, Phys. Rev. A **56**, R2499 (1997).
- ²²T. Beier, I. Lindgren, H. Persson, S. Salomonson, P. Sunnergren, H. Häffner, and N. Herrmannspahn, Phys. Rev. A **62**, 032510 (2000).
- ²³T. Beier, Phys. Rep. **339**, 79 (2000).
- ²⁴V. A. Yerokhin, P. Indelicato, and V. M. Shabaev, Phys. Rev. Lett. **89**, 143001 (2002).
- ²⁵V. A. Yerokhin, P. Indelicato, and V. M. Shabaev, Phys. Rev. A **69**, 052503 (2004).

- ²⁶V. A. Yerokhin and U. D. Jentschura, Phys. Rev. Lett. **100**, 163001 (2008).
- ²⁷V. A. Yerokhin and U. D. Jentschura, Phys. Rev. A **81**, 012502 (2010).
- ²⁸S. G. Karshenboim, V. G. Ivanov, and V. M. Shabaev, Can. J. Phys. **79**, 81 (2001); Zh. Eksp. Teor. Fiz. **120**, 546 [Sov. Phys. JETP **93**, 477](2001).
- ²⁹S. G. Karshenboim and A. I. Milstein, Phys. Lett. B **549**, 321 (2002).
- ³⁰R. N. Lee, A. I. Milstein, I. S. Terekhov, and S. G. Karshenboim, Phys. Rev. A **71**, 052501 (2005).
- ³¹K. Pachucki, U. D. Jentschura, and V. A. Yerokhin, Phys. Rev. Lett. **93**, 150401 (2004); ibid **94**, 229902(E)(2005).
- ³²K. Pachucki, A. Czarnecki, U. D. Jentschura, and V. A. Yerokhin, Phys. Rev. A **72**, 022108 (2005).
- ³³U. D. Jentschura, Phys. Rev. A **79**, 044501 (2009).
- ³⁴V. A. Yerokhin and Z. Harman, Phys. Rev. A **88**, 042502 (2013).
- ³⁵H. A. Bethe and E. E. Salpeter, *Quantum Mechanics of One- and Two-Electron Atoms* (Springer-Verlag, Berlin, 1957).
- ³⁶H. Grotch and R. A. Hegstrom, Phys. Rev. A **4**, 59 (1971).
- ³⁷K. Pachucki, Phys. Rev. A **78**, 012504 (2008).
- ³⁸M. I. Eides and T. J. S. Martin, Phys. Rev. Lett. **105**, 100402 (2010).
- ³⁹V. M. Shabaev, Phys. Rev. A **64**, 052104 (2001).
- ⁴⁰A. Yelkhovsky, arXiv:hep-ph/0108091(2001).
- ⁴¹V. M. Shabaev and V. A. Yerokhin, Phys. Rev. Lett. **88**, 091801 (2002).
- ⁴²D. A. Glazov and V. M. Shabaev, Phys. Lett. A **297**, 408 (2002).
- ⁴³S. G. Karshenboim, Phys. Lett. A **266**, 380 (2000).
- ⁴⁴S. G. Karshenboim, R. N. Lee, and A. I. Milstein, Phys. Rev. A **72**, 042101 (2005).
- ⁴⁵J. Zatorski, N. S. Oreshkina, C. H. Keitel, and Z. Harman, Phys. Rev. Lett. **108**, 063005 (2012).
- ⁴⁶A. V. Nefiodov, G. Plunien, and G. Soff, Phys. Rev. Lett. **89**, 081802 (2002).
- ⁴⁷A. V. Volotka and G. Plunien, Phys. Rev. Lett. **113**, 023002 (2014).
- ⁴⁸U. D. Jentschura, A. Czarnecki, K. Pachucki, and V. A. Yerokhin, Int. J. Mass Spectrom. **251**, 102 (2006).
- ⁴⁹T. Beier, H. Häffner, N. Hermanspahn, S. G. Karshenboim, H.-J. Kluge, W. Quint, S. Stahl, J. Verdú, and G. Werth, Phys. Rev. Lett. **88**, 011603 (2002).
- ⁵⁰P. J. Mohr, B. N. Taylor, and D. B. Newell, Rev. Mod. Phys. **84**, 1527 (2012).

- ⁵¹D. A. Glazov, V. M. Shabaev, I. I. Tupitsyn, A. V. Volotka, V. A. Yerokhin, G. Plunien, and G. Soff, Phys. Rev. A **70**, 062104 (2004).
- ⁵²D. A. Glazov, A. V. Volotka, V. M. Shabaev, I. I. Tupitsyn, and G. Plunien, Phys. Lett. A **357**, 330 (2006).
- ⁵³A. V. Volotka, D. A. Glazov, V. M. Shabaev, I. I. Tupitsyn, and G. Plunien, Phys. Rev. Lett. **103**, 033005 (2009).
- ⁵⁴D. A. Glazov, A. V. Volotka, V. M. Shabaev, I. I. Tupitsyn, and G. Plunien, Phys. Rev. A **81**, 062112 (2010).
- ⁵⁵A. V. Volotka, D. A. Glazov, G. Plunien, and V. M. Shabaev, Ann. Phys. (Berlin) **525**, 636 (2013).
- ⁵⁶A. V. Volotka, D. A. Glazov, V. M. Shabaev, I. I. Tupitsyn, and G. Plunien, Phys. Rev. Lett. **112**, 253004 (2014).
- ⁵⁷I. I. Tupitsyn, V. M. Shabaev, J. R. Crespo López-Urrutia, I. Draganić, R. Soria Orts, and J. Ullrich, Phys. Rev. A **68**, 022511 (2003).
- ⁵⁸I. I. Tupitsyn, A. V. Volotka, D. A. Glazov, V. M. Shabaev, G. Plunien, J. R. Crespo López-Urrutia, A. Lapierre, and J. Ullrich, Phys. Rev. A **72**, 062503 (2005).
- ⁵⁹V. M. Shabaev, I. I. Tupitsyn, K. Pachucki, G. Plunien, and V. A. Yerokhin, Phys. Rev. A **72**, 062105 (2005).
- ⁶⁰A. Wagner, S. Sturm, F. Köhler, D. A. Glazov, A. V. Volotka, G. Plunien, W. Quint, G. Werth, V. M. Shabaev, and K. Blaum, Phys. Rev. Lett. **110**, 033003 (2013).
- ⁶¹I. Angeli and K. P. Marinova, At. Data Nucl. Data Tables **99**, 69 (2013).
- ⁶²G. Werth, H. Häffner, N. Hermanspahn, H.-J. Kluge, W. Quint, and J. Verdú, *The g Factor of Hydrogenic Ions: A Test of Bound State QED* (in The Hydrogen Atom, Ed. by S.G. Karshenboim *et al.*, p. 204, Springer, Berlin, 2001).
- ⁶³D. L. Moskovkin, N. S. Oreshkina, V. M. Shabaev, T. Beier, G. Plunien, W. Quint, and G. Soff, Phys. Rev. A **70**, 032105 (2004).
- ⁶⁴D. L. Moskovkin and V. M. Shabaev, Phys. Rev. A **73**, 052506 (2006).
- ⁶⁵D. L. Moskovkin, V. M. Shabaev, and W. Quint, Opt. Spectrosc. **104**, 637 (2008).
- ⁶⁶D. L. Moskovkin, V. M. Shabaev, and W. Quint, Phys. Rev. A **77**, 063421 (2008).
- ⁶⁷V. A. Yerokhin, K. Pachucki, Z. Harman, and C. H. Keitel, Phys. Rev. Lett. **107**, 043004 (2011).
- ⁶⁸V. A. Yerokhin, K. Pachucki, Z. Harman, and C. H. Keitel, Phys. Rev. A **85**, 022512 (2012).
- ⁶⁹W. Quint, D. L. Moskovkin, V. M. Shabaev, and M. Vogel, Phys. Rev. A **78**, 032517 (2008).
- ⁷⁰M. Vogel and W. Quint, Phys. Rep. **490**, 1 (2010).

- ⁷¹D. von Lindenfels, N. P. M. Brantjes, G. Birkl, W. Quint, V. M. Shabaev, and M. Vogel, Can. J. Phys. **89**, 79 (2011).
- ⁷²D. von Lindenfels, M. Wiesel, D. A. Glazov, A. V. Volotka, M. M. Sokolov, V. M. Shabaev, G. Plunien, W. Quint, G. Birkl, A. Martin, and M. Vogel, Phys. Rev. A **87**, 023412 (2013).
- ⁷³M. Vogel and W. Quint, Ann. Phys. (Berlin) **525**, 505 (2013).
- ⁷⁴D. A. Glazov, A. V. Volotka, A. A. Schepetnov, M. M. Sokolov, V. M. Shabaev, I. I. Tupitsyn, and G. Plunien, Phys. Scr. **T156**, 014014 (2013).
- ⁷⁵V. A. Yerokhin, P. Indelicato, and V. M. Shabaev, Eur. Phys. J. D **25**, 203 (2003).
- ⁷⁶V. A. Yerokhin, Phys. Rev. A **80**, 040501(R) (2009).